microbial biotechnology

Open Access

Characterization of *Rhodopseudomonas palustris* population dynamics on tobacco phyllosphere and induction of plant resistance to *Tobacco mosaic virus*

Pin Su,[1†] Deyong Zhang,[1†] Zhuo Zhang,[1] Ang Chen,[1] Muhammad Rizwan Hamid,[1] Chenggang Li,[1] Jiao Du,[1] Ju'e Cheng,[1] Xinqiu Tan,[1] Limin Zhen,[1] Zhongying Zhai,[1] Wen Tang,[1] Jin Chen,[2] Xuguo Zhou[3] and Yong Liu[1]*

[1]*Hunan Plant Protection Institute, Hunan Academy of Agricultural Sciences, Changsha 410125, China.*
[2]*College of Bioscience and Biotechnology, Hunan Agricultural University, Changsha 410128, China.*
[3]*Department of Entomology, University of Kentucky, Lexington, KY 40546, USA.*

Summary

Although many biocontrol bacteria can be used to improve plant tolerance to stresses and to promote plant growth, the hostile environmental conditions on plant phyllosphere and the limited knowledge on bacterial colonization on plant phyllosphere minimized the beneficial effects produced by the biocontrol bacteria. *Rhodopseudomonas palustris* strain GJ-22 is known as a phyllosphere biocontrol agent. In this paper, we described detailed processes of strain GJ-22 colony establishment at various colonization stages. Four different types of bacterial colonies, Type 1, scattered single cells; Type 2, small cell clusters; Type 3, small cell aggregates; and Type 4, large cell aggregates, were observed in the course of bacterial colonization. We categorized bacterial colonization into four phases, which were, Phase I: bacterial colony exists as Type 1 and cell population reduced quickly; Phase II: Type 1 evolved into Type 2 and cell population remained steady; Phase III: Type 3 arose and replaced Type 2, and cell population expanded slowly; and Phase IV: Type 3 matured into Type 4 and cell population increased quickly. We have shown that the preferable location sites of bacterial aggregates on leaf phyllosphere are grooves between plant epidermal cells. Analyses of expressions of plant defence-related genes showed that, starting from Phase III, bacterial cells in the Type 3 and Type 4 colonies produced unidentified signals to induce host defence against *Tobacco mosaic virus* infection. In addition, we determined the crucial role of aggregates formation of GJ-22 cell on plant phyllosphere in terms of bacterial cell stress tolerance and ISR (induced systemic resistance) priming. To our knowledge, this is the first report focused on the colonization process of a phyllosphere biocontrol agent and gave a clear description on the morphological shift of bacterial colony on phyllosphere.

Introduction

Phyllosphere, also known as aerial part of plant, is the first-line plants used to fight against pathogen infections (Berg, 2009; Natacha *et al*., 2014). Phyllosphere also provides an ideal habitat for bacterial species that are beneficial to plant growth and stress tolerance (Vorholt, 2012; Kembel *et al*., 2014; Duke *et al*., 2017). Successful applications of microbes with biocontrol activities to plant phyllosphere are crucial for effective crop disease managements (Kim *et al*., 2011; Lambais *et al*., 2014). The most commonly used microbes with biocontrol activities are plant growth-promoting rhizobacteria (PGPR), and the best-known PGPRs are those currently being used to control crop soil-borne diseases (Bulgarelli *et al*., 2013; Hassani *et al*., 2018). Introduction of PGPRs to plant phyllosphere is not easy, due mainly to the hostile environments, including limited nutrients, limited water supply, UV radiation and toxic substances secreted by plants or produced by other microbes (Lindow and Brandl, 2003; Müller *et al*., 2016). These hostile conditions can dramatically affect PGPR survival and population density in field. Earlier studies had indicated that inhibition of beneficial microbe growth could lead to much lower microbial population density on leaf phyllosphere and thus significantly reduce the beneficial

Received 14 May, 2019; revised 16 August, 2019; accepted 26 August, 2019.
*For correspondence. E-mail haoasliu@163.com; Tel. 86-0731-84691176; Fax 86-0731-84696578.
†Co-first author.
Microbial Biotechnology (2019) **12**(6), 1453–1463
doi:10.1111/1751-7915.13486
Funding information
This research was supported by the National Key R&D Program of China (2017YFD0200400), the National Science Foundation of China (31701764), Hunan Agricultural Science and Technology Innovation Fund (2017GC04), Hunan Natural Science Foundation (2017JJ3169), and the Hunan Provincial key research and Development Plan (2016NK2199).

effects caused by PGPR (Bonaterra *et al*., 2007). However, studies on bacterial colonization on leaf phyllosphere are mostly from plant pathogenic bacteria such as *Pseudomonas syringae* (Haefele and Lindow, 1987) and *Erwinia* (*Pantoea*) spp. (Okinaka *et al*., 2002). The current knowledge on PGPR colonization on leaf phyllosphere is very limited.

Rhodopseudononas palustris is a purple non-sulphur photosynthetic bacteria in Class *Alpha-proteobacteria*, Phylum *Proteobacteria*. Strains of *R. palustris* are often known as free-living bacteria in soils or in aquatic sediments (Larimer *et al*., 2004). Strains of this bacterium had drawn enormous interests from researchers who are interested in *R. palustris* metabolic abilities, including nitrogen fixation, hydrogen gas production, and degradation of aromatic compounds and chlorinated pollutants (Sasaki *et al*., 2005). *R. palustris* is now widely used to treat agricultural and industrial wastes or to produce bioenergy (Idi *et al*., 2015). Its potentials in organic farming are new topics of many research laboratories (Fawzy *et al*., 2012; Wu *et al*., 2013; Wong *et al*., 2014). In our previous report, we have shown that *R. palustris* GJ-22 strain can induce a systemic resistance (referred to induced systemic resistance [ISR] thereafter) to *Tobacco mosaic virus* (TMV) infection in tobacco and promote plant growth through production of two phytohormones (i.e. indole-3-acetic acid and 5-aminolevulinic acid; Su *et al*., 2017).

Unlike many other PGPR strains that colonize plant rhizosphere, *R. palustris* GJ-22 can colonize plant phyllosphere and establish different-sized colonies to exert beneficial effects to plant. After being introduced to tobacco phyllosphere, the population density of *R. palustris* GJ-22 declined quickly and then recovered to form large-sized colonies. This phenomenon suggests that *R. palustris* GJ-22 utilizes some as yet unidentified strategies to overcome biotic and abiotic stresses during its colonization on plant phyllosphere. Bacterial exopolysaccharide (EPS) production is one of the most studied aspects related to the bacteria epiphytic fitness. Exopolysaccharides are the major ingredients promoting bacterial aggregate formations and act as molecular glue for adhesions between bacterial cells, and bacterial cells to plant phyllosphere (Limoli *et al*., 2015). Formation of aggregates can benefit bacterial survival under biotic and/or abiotic stresses (Vorholt, 2012). It is possible that *R. palustris* GJ-22 may use this strategy to survive the phyllosphere condition. Strains of *R. palustris* are often referred to as free-living bacteria in soils or in aquatic sediments. Current knowledge on *R. palustris* lifestyle is largely from the soil or aquatic *R. palustris* strains. There is little known about how *R. palustris* adapt to phyllosphere conditions.

In this study, we investigated the formation of bacterial colony on tobacco leaves inoculated with strain GJ-22-eGFP, a modified GJ-22 strain expressing the green fluorescent protein, using both laser scanning confocal microscopy (LSCM) and scanning electron microscopy (SEM). We found that *R. palustris* strain GJ-22 could form Type 3 (small aggregate) colony by 72 h post-bacterial inoculation and Type 4 (large aggregate) colony by 96 h post-bacterial inoculation on leaf phyllosphere. *R. palustris* GJ-22 cells inside the Type 3 and 4 colonies were able to induce ISR in tobacco to *Tobacco mosaic virus* (TMV) infection. The findings presented here provide useful information on the establishment of *R. palustris* colonies on leaf phyllosphere and information needed for the development of new strategies using this biocontrol agent.

Results

Population dynamic and strain GJ-22 colony morphology on N. benthamiana *phyllosphere*

In order to determine how GJ-22 colonizes plant leaves over time, we inoculated *N. benthamiana* leaves with a GJ-22 suspension at 6×10^7 CFU ml^{-1} and followed its population size over time (population dynamic) for 96 h. Analysis of population dynamic of *R. palustris* strain GJ-22 on *N. benthamiana* phyllosphere demonstrated that strain GJ-22 took 96 h to reach full population size (Fig. 1A). Within the first 24 h, the population size dropped from 5.3×10^7 CFU ml^{-1} to 4.8×10^3 CFU ml^{-1}. This population size maintained for at least 24 h and then increased from 68 hpi (3.14×10^4 CFU ml^{-1}) to 84 hpi (4.63×10^6 CFU ml^{-1}). This steady increase continued in the following 12 h and reached to 9.7×10^6 CFU ml^{-1} by the 96 hpi. The population dynamic can be summarized as a dramatic decline during early growth stage followed by a static state, a slow increase and then a rapid increase (Fig. 1A).

Analysis of green fluorescent signal produced by strain GJ-22-eGFP through LSCM or analysis of wild-type GJ-22 through SEM showed that the bacterial cells on phyllosphere formed four types of colonies during colony establishment (Fig. 1B). At the initial colonization state (0–20 hpi), bacterial cells were mostly seen as single cells randomly distributed on leaf surfaces. Representative images captured by LSCM or SEM at 12 hpi are shown as Type 1 in Fig. 2. Most of the single bacterial cells on leaf surfaces died over time, leading to a decrease of green fluorescent signal under LSCM. The cells lodged at the junctions between plant epidermal cells survived and multiplied afterwards. Between 20 and 48 hpi, the multiplied cells began to form small clusters at the junctions. Representative images captured at 48 hpi are shown as Type 2 in Fig. 2. Small clustered bacterial cells continued to grow and form aggregates during the next 24 h. Representative images captured at 72 hpi

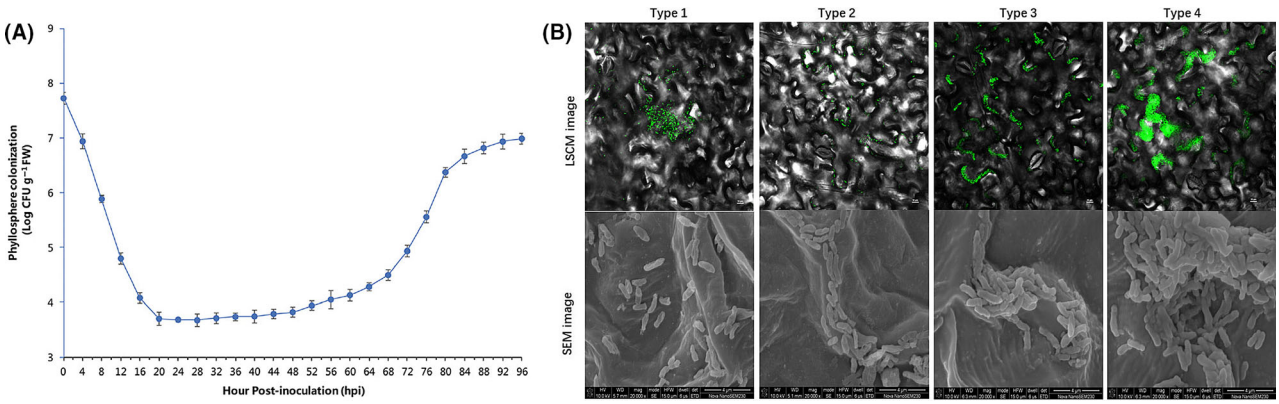

Fig. 1. Population dynamic, distributions and colony morphology of *R. palustris* strain GJ-22 on *N. Benthamiana* phyllosphere. A. *R. palustris* strain GJ-22 was inoculated onto *N. Benthamiana* leaves. Population densities of strain GJ-22 on *N. Benthamiana* phyllosphere were examined at 4 h intervals from 0 ~ 96 hpi. The plant growth conditions were set at 28°C, 16/8 h (light/dark) photoperiod, and 85% relative humidity. The data were presented as the means from four biological repeats. Error bars represented the standard deviation. B. The GFP fluorescent produced by GJ-22-eGFP, a wild type GJ-22 harboring an eGFP gene, was sprayed onto *N. Benthamiana* leaves. Images of bacterial cells were captured by LSCM (upper panel) or SEM (lower panel) at 12 hpi (Type 1), 48 hpi (Type 2), 72 hpi (Type 3) and 96 hpi (Type 4), respectively. Bars in upper panel = 10 μm, bars in lower panel = 4 μm.

are presented as Type 3 in Fig. 2. The cell aggregates enlarged rapidly to form large aggregates. By 96 hpi, the bacterium existed mostly as large aggregates. Representative images captured at 96 hpi are presented as Type 4 in Fig. 2. At this time point, bacterial colonies were no longer confined at the junctions between plant epidermal cells but expanded to the surrounding surfaces. In summary, four different types of bacterial colonies, Type 1, scattered single cells; Type 2, small cell clusters; Type 3, small cell aggregates; and Type 4, large cell aggregates, were observed in this study.

To further illustrate colony dynamics from Type 1 to Type 4, we calculated the percentage of leaf samples showing each colony type (Fig. 2). In the early stage of colonization (0~20 hpi), over 70% leaf sample had the Type 1 colonies. Type 2 colonies started to appear at 16 hpi, and by 48 hpi, 72% leaf sample had Type 2 colonies while the Type 1 colony was observed in only about 8% leaf samples. The number of Type 2 colony started to decrease afterwards and the Type 3 colony started to emerge. By 72 hpi, about 60% leaf sample contained Type 3 colonies while only 6% leaf sample contained Type 2 colonies. By 96 hpi, about 60% leaf sample contained Type 4 colonies while only 4% leaf sample contained Type 3 colonies (Fig. 2).

Formation of aggregates enhanced strain GJ-22 tolerance to drought and heat stresses

To investigate whether formation of bacterial aggregate could enhance GJ-22 tolerance to stresses, we treated bacterial cells in different colony types with drought and heat stresses. *N. benthamiana* seedlings were inoculated with GJ-22-eGFP cells and then grown under the normal

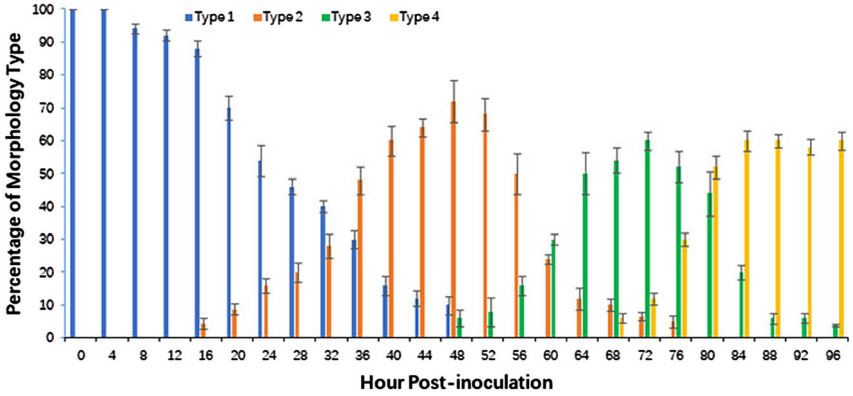

Fig. 2. Morphological changes from Type 1 colony to Type 4 colony during the colony establishment. GJ-22-eGFP cells were sprayed onto *N. Benthamiana* leaves. The inoculated leaves were collected at 4 h intervals from 0 ~ 96 hpi. Fifteen leaf discs (2 × 2 mm) were randomly sampled from leaves of each plant (three plants per treatment). The collected leaf samples were examined for bacterial colony morphology by LSCM. The number of samples carrying a specific colony type was recorded and used to calculate the percentage of samples with a specific colony type. The results are presented as the mean percentage ± standard deviation.

growth condition (Fig. 3A). After 12 h (leaves contained mostly Type 1 colonies), 48 h (leaves contained Type 2 colonies), 72 h (leaves contained mostly Type 3 colonies) and 96 h (leaves contained mostly Type 4 colonies), the inoculated plants (4 plant per time point) were transferred to stressed condition (relative humidity = 40%, temperature = 39°C). The stressed plants were sampled and examined by LSCM. Results showed that the Type 3 and Type 4 colonies maintained their morphology after 1 or 3 day stress treatment (Fig. 3A). The Type 1 and Type 2 colonies died rapidly after the treatment. Analysis of population densities after the stress treatment showed that cells in the Type 3 and Type 4 colonies were more tolerant to drought and heat stresses than the cells in the Type 1 and Type 2 colonies, based on the drastic cell density drop in Type 1 and Type 2 colony and the cell density in Type 3 and Type 4 colony maintained at similar level after stress treatment (Fig. 3B).

R. palustris *strain GJ-22 primed ISR in plants after aggregate formation on phyllosphere*

Timing of ISR onset during strain GJ-22 colonization process was investigated. The GJ-22-eGFP inoculated seedlings were grown under the normal condition for 12, 48, 72 or 96 h to produce Type 1, Type 2, Type 3 and Type 4 colonies (Fig. 4A). After removal of the inoculated leaves, the assayed plants were inoculated with purified TMV (Fig. 4A). Accumulation of TMV in the inoculated plants was determined through ELISA at 6 dpi, to evaluate the ISR against TMV. In the plants that had Type 3 or Type 4 GJ-22 colonies, the accumulation levels of TMV were 52 and 67.4% lower than that in the plants without *R. palustris* strain GJ-22 inoculation (mock; Fig. 4B). For plants that had Type 1 and Type 2 colonies, the accumulation levels of TMV were similar to that in the mock control plants. We then analysed the expressions of *NbPR1a* and *NbPR3* in plants at 18 h post-TMV inoculation to validate the onset of ISR (Fig. 4C). The plants with Type 3 or Type 4 colonies showed quicker upregulations of *NbPR1a* and *NbPR3* expressions compared with the mock plants or the plants had Type 1 or Type 2 colonies, suggesting that strain GJ-22 had the ability to prime ISR in plants after formation of Type 3 and Type 4 colonies.

Formation of aggregates played a vital role in GJ-22 cell tolerance to drought and heat stresses and ISR priming in plants

Exopolysaccharides (EPSs) are the major ingredients promoting bacterial aggregate formations. Compromised EPS production can result in failure of bacterial aggregate formation. Based on the GJ-22 genome, we identified two polysaccharide biosynthesis/export protein genes, here designated as *Exop1* and *Exop2*. Mutation of the *Exop1* gene significantly reduced the EPSs production in culture condition. The mutant *ΔExop1* produced 69% less EPSs than wild-type strain did, and no significant decrease of EPSs production was detected in *ΔExop2* (Fig. 5A). Inoculation of *ΔExop1* on plant phyllosphere did not produce Type 3 colony as wild type did (Fig. 5B) when leaf

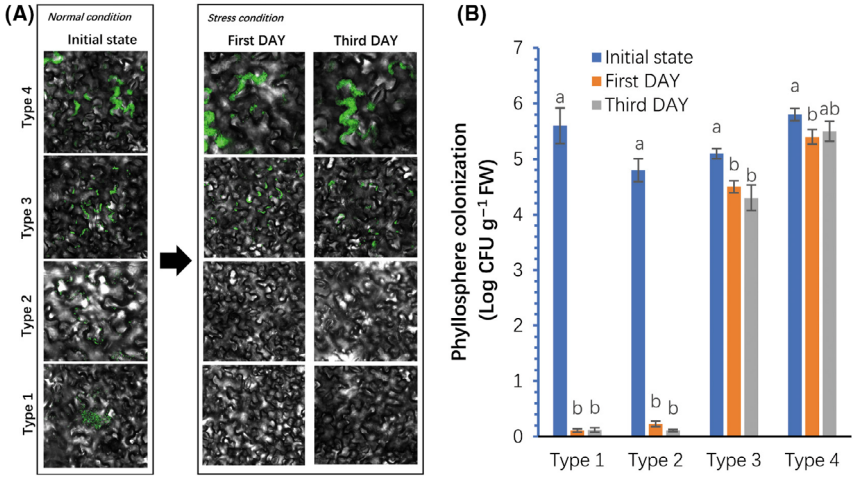

Fig. 3. Stress tolerance of strain GJ-22 in different types of colonies on *N. Benthamiana* phyllosphere. A. LSCM images of strain GJ-22-eGFP on *N. benthamiana* phyllosphere under different growth conditions. Bacterial cells on the plants grown under the normal conditions were labeled as initial stage. Representative images of GJ-22-eGFP on plant phyllosphere at 12 (Type 1), 48 (Type 2), 72 (Type 3), and 96 (Type 4) hpi are shown. After being grown under the normal condition, the plants were grown under the stress conditions for three days before LSCM. Images were taken from these plants at one or three days post stress treatment. B. Population density of *strain* GJ-22 on *N. benthamiana* phyllosphere under different growth conditions. Population density was determined at the initial state, and first and third day post stress treatment. The data presented were the means ± standard deviations from four biological replicates per treatment. Different small letters above the bars indicate the statistical difference between treatments within the same group by the Fisher's LSD (P = 0.05).

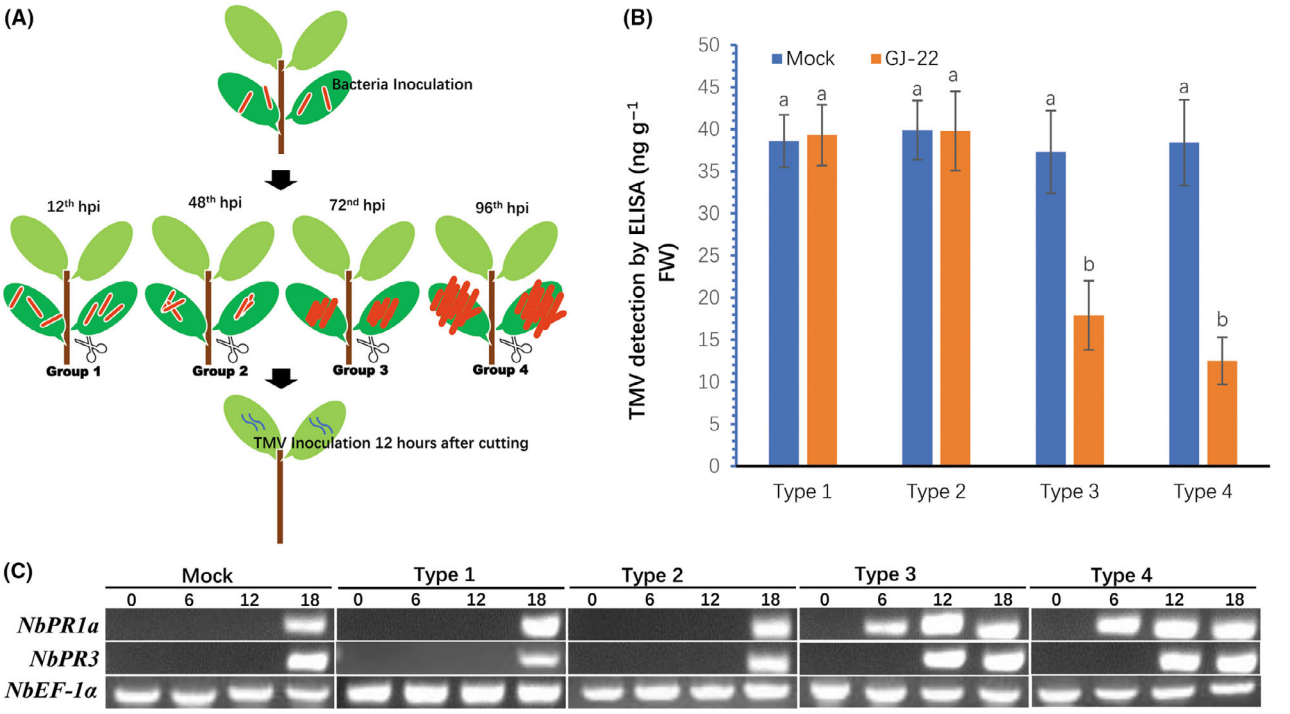

Fig. 4. Priming ISR onset by *R. palustris* strain GJ-22 in *N. benthamiana* plants. A. A schematic diagram showing experimental design. The fifth and sixth leaves of *N. benthamiana* plants were sprayed with bacterial strain GJ-22 suspension. After detachment of the sprayed leaves at 12, 48, 72 or 96 hpi, the plants were inoculated with TMV. The TMV inoculated leaves were harvested at 6 dpi. B. Accumulation of TMV in the inoculated leaves was determined by ELISA. The results were presented as the means ± standard deviations from four biological replicates per treatment. Different small letters above the bars indicate statistical differences between treatments in each group by the Fisher's LSD (P = 0.05). C. Induction of *NbPR1a* and *NbPR3* expressions in the TMV-inoculated leaves. The TMV-inoculated leaves were harvested at various hpi and analyzed by semi-quantitative RT-PCR followed by electrophoresis. The expression of *NbEF-1α* was used as an internal control. Similar results were obtained in three parallel experiments.

samples were observed under SEM at 72 hpi. Those results indicated that GJ-22 relied on polysaccharide biosynthesis/export protein Exop1 to produce EPSs and form aggregates *in planta*. To assess the essential role of aggregate formation of GJ-22 cell in plant phyllosphere for the bacterial cell tolerance to stress and ISR priming in plants, we compared the cell survival under stress conditions and the generation of ISR against TMV between wild type and *ΔExop1*. Three days after bacterial inoculation, plants with wild type and *ΔExop1* were transferred to stress growth condition. The *ΔExop1* exhibited vulnerability to stress conditions. By the time of 5th and 7th dpi, the phyllosphere colonization of *ΔExop1* dropped to 6.3×10^2 CFU g^{-1} FW and 2.3×10^1 CFU g^{-1} FW, significantly lower than that of wild type (Fig. 5C). The *ΔExop1* also showed significant decrease in protecting plants against TMV in comparison with wild type. Accumulation level of TMV in *ΔExop1* inoculated plants was 85% higher than that in the plants with wild type (Fig. 5D).

Discussion

In this report, we have demonstrated that after attachment to tobacco phyllosphere, *R. palustris* strain GJ-22 underwent a gradual change of colony morphology, starting from Type 1 colony to Type 4 colony. The change from Type 1 to Type 2 colony took about 36 h, and change from Type 2 to Type 3 colony or Type 3 to Type 4 about 24 h. In addition, colony morphology change accompanied with specific bacterial population densities. For example, change from Type 1 to Type 2 colony occurred during the static state of bacterial growth while the change from Type 2 to Type 3 colony occurred during the bacterial slow growth stage. When strain GJ-22 started to grow rapidly on tobacco leaf phyllosphere, Type 4 colony became to appear. Based on these findings, we characterized strain GJ-22 colonization on leaf phyllosphere into four different phases (Fig. 6). In the phase I stage, individual strain GJ-22 cells are randomly distributed across the leaf surface. These cells die quickly, due mainly to environmental stresses, leading to quick reduction of cell population and colony size. In phase II stage, strain GJ-22 cells started to form small clusters located at the junctions between plant epidermal cells. At this stage, bacterial cell population density remained steady and at the lowest level. In the phase III stage, strain GJ-22 cell clusters started to expand and formed small aggregates at the

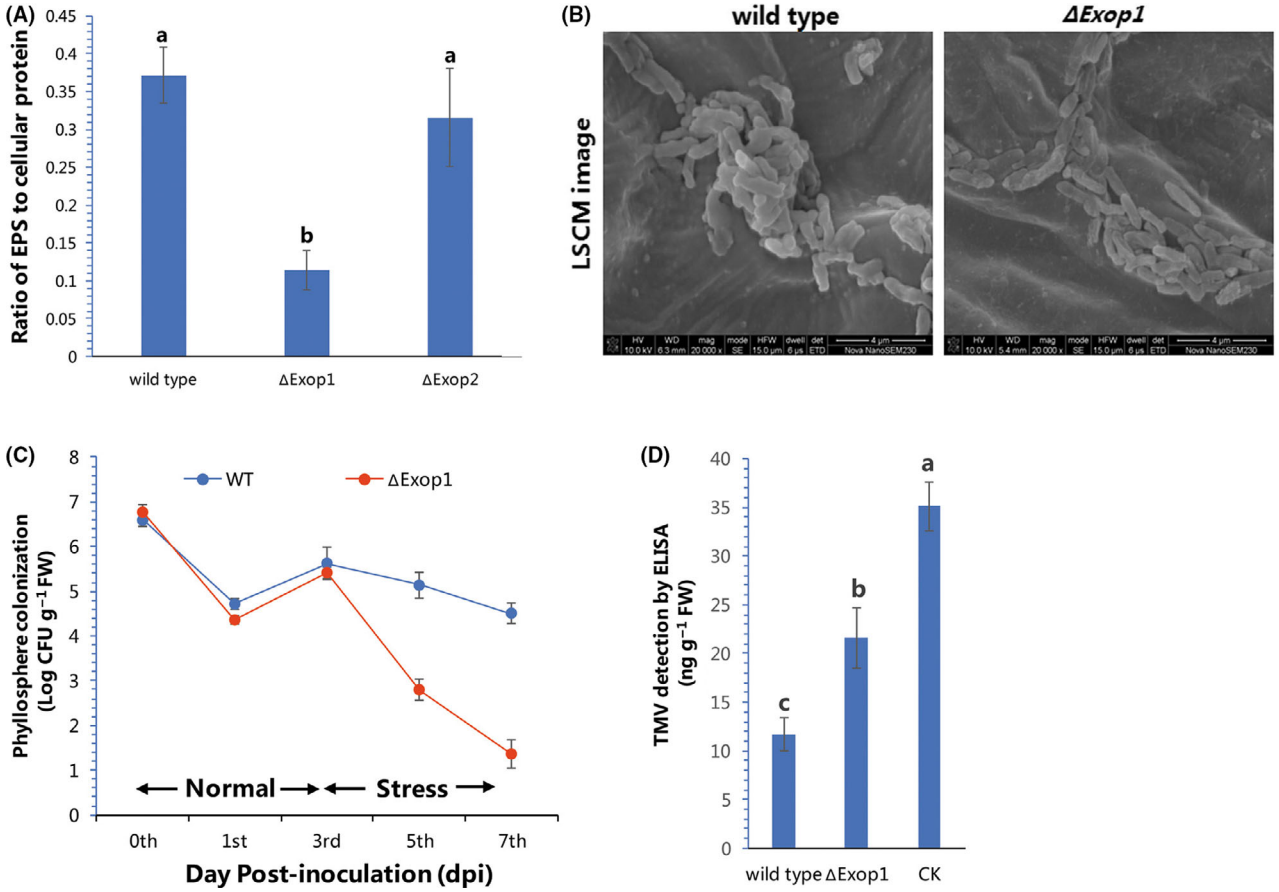

Fig. 5. Formation of aggregates is vital for stress tolerance and ISR priming of *R. palustris* strain GJ-22 in *N. benthamiana* plants. A. The EPSs production of wild type, *ΔExop1* and *ΔExop2*. Culture samples were taken at 6 dpi and the amount of EPSs in each sample was presented as a ratio between the amount of EPSs and the amount of cellular protein. B. Bacterial colony morphology by SEM. Representative images of wild type and *ΔExop1* on plant phyllosphere at 72 hpi are shown. Bars in panel = 4 μm. C. Colonization of wild type, *ΔExop1* cells in plant phyllosphere under stress growth conditions. D. Accumulation of TMV in the wild type or *ΔExop1*-inoculated leaves was determined by ELISA. CK stands for the mock control by spraying plant leaves with PPB. The results were presented as the means ± standard deviations from four biological replicates per treatment. Different small letters above the bars indicate statistical differences between treatments in each group by the Fisher's LSD (P = 0.05).

junctions between plant epidermal cells. Bacterial cells in small aggregates or small colonies started to produce unidentified substances that could enhance plant tolerance to biotic and abiotic stresses. The size of bacterial aggregate or colony continued to expand slowly in this phase. In the phase IV stage, the bacterium formed large aggregates or colonies on leaf phyllosphere and the size of bacterial colony continued to expand due to rapid cell multiplications. By the end of this phase, bacterial aggregates started to emerge to form very large aggregates or colonies, companied with an significant increase of bacterial population density.

Phyllosphere bacteria form different-sized aggregates or colonies at the junctions between plant epidermal cells or at the junctions along the veins or at the base of leaf trichrome (Beattie and Lindow, 1999). In this study, we observed that the preferential colonization location of strain GJ-22 was at the junctions between plant epidermal cells. In the early growth stages, most bacterial cells on leaf phyllosphere showed desiccation and then died. We speculate that the environment at the grooves formed by plant leaf epidermal cells provides bacterial cells a shelter with sufficient nutrients and water to survive and later to grow. Since the spaces provided by these grooves for bacteria growth are limited, most bacterial cells applied to plant canopy quickly desiccated and died. The survived cells started to multiply very slowly at the early colonization stage followed by a moderate multiplication to form Type 3 colonies. After entering the Phase III stage, the bacterial aggregates started to form its own microenvironments to capture nutrients from plant exudates, to maintain water within microenvironments, and to protect bacterial cells from lytic enzymes and/or toxic substances produced by plant or other microbes. This strategy is commonly used by phyllosphere epiphytes (Wilson *et al.*, 1999; Bulgarelli

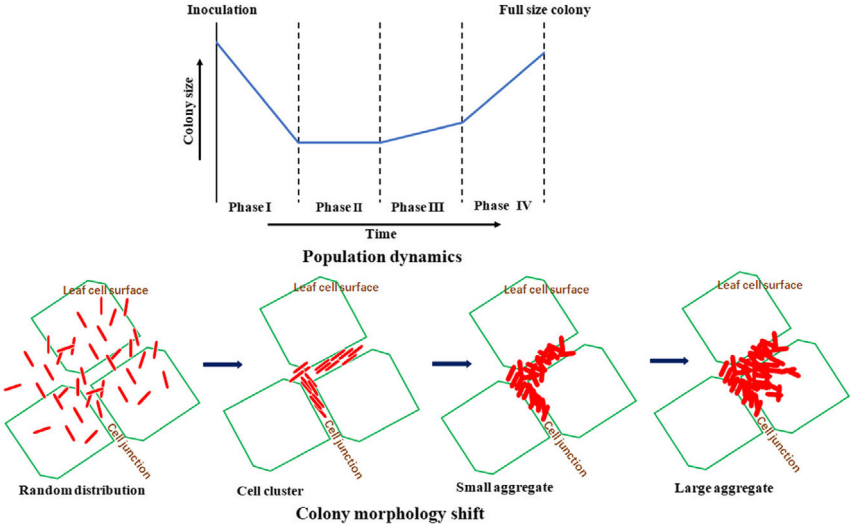

Fig. 6. Colonization of *Rhodopseudomonas palustris* strain GJ-22 on leaf phyllosphere.

et al., 2013; Remus-Emsermann and Schlechter, 2018) and can be used to explain the increased stress tolerance of strain GJ-22 after the Phase III stage.

Exopolysaccharides (EPSs) are the major ingredients mediating the adhesion between bacterial cells on plant surfaces to form bacterial aggregates (Limoli *et al*., 2015). EPSs can also provide protection to bacterial cells from various stresses. Production of EPSs was reported to be controlled via a cell-density-dependent manner known as quorum sensing (QS) in many Gram-negative bacteria (Marketon *et al*., 2003; Tan *et al*., 2014). Quorum sensing is a process used by bacteria to monitor their local population density and to regulate gene expressions at different population densities. Many Gram-negative bacteria also use QS to regulate their colony morphology that are vital for successful bacterial colonization and habitat modification on plants (Quiñones *et al*., 2004, 2005). It was suggested that when bacterial cell density at the Phase II stage reached a certain threshold, the QS system started to upregulate EPS production to facilitate aggregate formation. *R. palustris* was reported to possess a *rpaI-rpaR* gene pair-based QS system (Schaefer *et al*., 2008). The rpaI protein utilizes a plant-produced *p*-coumarate to synthesize a *p*-coumaroyl-homoserine lactone (*p*C-HSL) signal (Lindemann *et al*., 2011; Hidetada *et al*., 2012). To date, how *rpaI-rpaR* gene pair-based QS system regulates EPS production in *R. palustris* is unknown. The availability of nutrients on plant phyllosphere is likely the major determinant of epiphytic colonization. Numerous evidence has indicated that plant epiphytes can modify their habitats through modification of nutrient concentrations on plant surfaces (Beattie and Lindow, 1999). The size expansion of strain GJ-22 colonies at the Phase IV stage suggested a better nutrient condition during this phase. Strain GJ-22 was reported to produce IAA as a signal to promote plant growth (Su *et al*., 2017). This phytohormone was also reported to induce release of nutrients, including saccharides, from plant cells (Spaepen *et al*., 2007; Limtong and Koowadjanakul, 2012). We speculate that the formation of bacterial aggregates may upregulate IAA production in *R. palustris* and later infiltrate into plant cells. Notably, the GJ-22-triggered ISR in *N. benthamiana* mobilized both SA-responsive gene *NbPR1a* and JA/ET-responsive gene *NbPR3,* suggesting simultaneously activating SA- and JA/ET-dependent signalling pathways. Such type of ISR was also documented in *Arabidopsis thaliana* triggered by the plant growth-promoting rhizobacterium *Bacillus cereus* AR156 (Niu *et al*., 2011). In AR156-triggered ISR, the activating JA-signalling pathway was achieved by downregulating the transcription factor WRKY11 and activating SA-signalling pathway by upregulating WRKY70 (Jiang *et al*., 2015). Based on our findings, it can be speculated that GJ-22 may produce unique microbe-associated molecular patterns (MAMPs) recognized by *N. benthamiana,* leading to the generation of this distinct ISR.

In conclusion, the results obtained from this study revealed the process of *R. palustris* strain GJ-22 colony establishment. Because bacterial stress tolerance, the colony size expansion and priming of ISR in plant to TMV infection all occurred after the formation of large-sized bacterial colonies, it is likely that formation of bacterial aggregate has an important role on GJ-22 epiphytic fitness. Further investigations are needed to elucidate the mechanism(s) controlling aggregate formation. Our results can benefit the design of a better application method to deploy these bacteria to plant phyllosphere.

Experimental procedures

Bacterial strains, cultural conditions and plant inoculum

R. palustris strain GJ-22 was obtained from a previously reported source (Su *et al*., 2017) and routinely cultivated aerobically at 30°C in a photosynthetic medium (PM) under a 6500 lux illumination. The solid PM medium contains 0.1 g $(NH_4)_2SO_4$, 0.02 g $MgSO_4$, 0.5 g Na_2CO_3, 0.05 g K_2HPO_4, 0.02 g NaCl, 0.2 g casamino acids, 0.15 g yeast extract and 18 g agarose in one litre distilled water, pH 6.5–7.0. *Escherichia coli* DH5α was aerobically cultured in the Luria–Bertani (LB) broth at 30°C and used for plasmid propagations. *E. coli* S17-1 was cultured in the LB broth at 37°C and used as donor cells for conjugation. GJ-22 mutant strains were cultured in liquid PM medium with specific antibiotics as indicated.

The transformation of GJ-22 wild type with plasmid pBBR1MCS-2-pAMP-EGFP (Beijing TsingKe Biotech Co., Ltd., Beijing, China) was conducted through the following procedure. Cells were pelleted from liquid culture (OD660 = 0.4), rinsed three times with an ice-cold sterile water before resuspended in 10% glycerol solution, and resuspended cells were immediately stored at −80°C for later use. Electro-competent cell suspension (50 μl) was thawed on ice for 20 min, mixed with 5 ng plasmid DNA in a 2 mm Gene Pulser cuvette containing 80 μl ice-cold sterile water and incubated on ice for 10 min for incubation followed by electroporation using Eppendorf Eporator as described (Eppendorf North America, Hauppauge, NY, USA). The transformed cell suspension was transferred to 10 ml liquid medium and cultured for 20 h at 30°C with 6500 lux illumination inside a light incubator. The positive transformants were selected on agar medium with 50 μg ml^{-1} kanamycin under the same culture condition described above. Stability of the mutants was analysed by cultivating them individually in the liquid medium, with and without kanamycin, for 20 generations. For EGFP-labelled strain GJ-22-EGFP, the fluorescence shown by each generation was examined with a laser scanning confocal microscope (LSCM; Nikon C2 plus, Nikon, Japan). The excitation wavelength was set at 488 nm, and the emission wavelength was set at 522/35 nm.

GJ-22 mutants *ΔExop1* and *ΔExop2* were generated individually after replacing Exop1 (locus tag GJ-22_12270) or Exop2 (locus tag GJ-22_22975) coding sequence (CDS) with a cassette containing a CaMV 35S promoter-driven Hyg^r gene. The GJ-22 genome information was uploaded into GenBank (Accession Number: CP041387). The gene replacing mutations were conducted individually by conjugating GJ-22 with S17-1 transformed with a specific homologous recombinant suicide plasmid as described. The suicide plasmids used in this study include pSUP202E1 for Exop1 mutation and pSUP202E2 for Exop2 mutation. Names of bacterial strains and plasmids, and their characteristics are listed in Table S1. Primer sequences and their applications are listed in Table S2. Methods used for plasmid constructions, cell conjugations and electroporation are also described in the Appendix S1.

To prepare fresh bacterial culture, small amount of original cell stock culture (OD_{660} = 0.4) was added into a fresh liquid medium at the ratio of 1:20 (stock bacterium: medium, v/v). Before bacterial inoculation, GJ-22 and its mutants or GJ-22-eGFP culture were pelleted, resuspended in a 100 mM potassium phosphate butter (PPB), pH 7.2, and adjusted to 6×10^7 CFU ml^{-1} immediately prior to plant inoculation.

Plant growth and inoculation

Nicotiana. benthamiana seeds were sterilized by adding 70% ethanol solution for 30 min at room temperature (RT). After removing 70% ethanol by low-speed centrifugation, the seeds were treated with 100% ethanol for 15 min. The seeds were dried on filter papers for 1 h and geminated on wet filter papers at 25°C. The germinated seeds were individually transferred to pots (10 cm × 10 cm × 15 cm) containing pH-balanced peat moss (Klasmann-Deilmann GmbH, Geeste, Germany) inside a growth chamber set at 28°C, at 16/8 h (light/dark) photoperiod and 85% relative humidity. For stress assays, the growth chamber was set at 37°C, a 16/8 h (light/dark) photoperiod and 40% relative humidity. Bacterial inoculation was conducted by spraying 14-day-old *N. benthamiana* seedlings till the seedling became soaking wet. The inoculated seedlings were grown inside a growth chamber under the conditions described above.

Bacterial sampling and phyllosphere population density determination

Bacterial cells were collected at various hours post-inoculation (hpi) with the following method. The third and fourth leaves (down from the top) were harvested from individual assayed plants and pooled. Ten grams of tissues was sampled from each harvested leaf sample and submerged in 200 ml PPB inside a 500 ml conical flask. After 20 min, the samples were sonicated at 47 kHz for 10 min and with 150 r.p.m. shaking. Bacterial cells in each PPB solution were pelleted through 10 min centrifugation at 10 000 *g*. This procedure was repeated three times, and the bacteria-containing PPB solutions from each leaf sample were pooled. After centrifugation, the pelleted cells were resuspended in 2 ml PPB with 20% Percoll followed by 10 min centrifugation at 12 000 *g* to remove the remaining plant debris.

Bacterial population density in each sample was determined by plating the serially diluted bacteria-containing solutions on PM plates. The inoculated plates were then incubated for 6 days at 25°C, and the colony-forming unit (CFU) on each plate was counted and later converted to CFU g^{-1} FW (bacterial population size).

Assay of ISR onset in R. palustris *strain GJ-22 inoculated* N. benthamiana

PPB solution containing strain GJ-22 was sprayed onto the fifth and sixth leaf of *N. benthamiana* seedlings. Seedlings sprayed with equal amount of PPB only were used as controls. The sprayed leaves were detached from the plants at 12, 48, 72 and 96 hpi. At 12 h post-detachment, the third and fourth leaves of each seedling were mechanically inoculated with purified TMV (40 ng per leaf). The TMV-inoculated leaves were harvested at 6 days post-TMV inoculation and analysed for TMV accumulation by enzyme-linked immunosorbent assay (ELISA). To determine the expressions of defence-related genes, the TMV-inoculated leaves were harvested at 18 h post-TMV inoculation and the expressions of defence-related protein genes *NbPR1a and NbPR3* were analysed by semi-quantitative reverse transcription–polymerase chain reaction (RT-qPCR) as described previously (Su *et al*., 2017).

Exopolysaccharide (EPS) quantification

Total EPSs, including the unbound EPSs in the culture supernatant and the bound EPSs on cell surface, were quantified as described previously (Von Bodman *et al*., 1998) with minor modifications. Bacterial cells were cultured in 150 ml liquid PM in individual 500 ml conical flasks. EPS extraction was done at 6 dpi. Samples were collected from three cultures with similar OD660 values (variation ≤ 0.01) in three different flasks. The cell cultures were centrifuged to separate the cell pellets and supernatants. The supernatants were mixed individually with three volumes of absolute ethanol to precipitate the unbound EPSs. For bound PES, the cell pellets were resuspended individually in 50 ml high-salt buffer (i.e. 10 mM KPO_4, 15 mM NaCl, 1 mM $MgSO_4$ in distilled water, pH 7.0) and blended at 0°C for 30 min using a Mixer Mill MM400 (Retsch, Haan, Germany) set at Setting 2. After removing the cells from buffer by centrifugation, the supernatant was mixed with three volumes of absolute ethanol to precipitate the bound EPSs. The bound and unbound EPSs were pelleted from the ethanol solutions by 30 min centrifugation at 12 000 *g*. The EPS pellets were then individually resuspended in 10 ml sterile water followed by a phenol-sulphuric acid extraction prior to EPS quantifications. Different concentrations of D-glucose were used to generate a standard curve for the test, and all the samples were measured using a 96-well microplate reader set at 488 nm. Bacterial cells obtained in this study were also used for cellular protein content assays using the Bradford method**.** The amount of EPSs in each sample was presented as a ratio between the amount of EPSs and the amount of cellular protein.

Laser scanning confocal microscopy and scanning electron microscopy

For LSCM analysis, leaf tissues were collected and cut into 2 × 2 mm pieces. Bacterial cells on the surface of each leaf sample were examined under a Nikon epifluorescence microscope confocal system (Nikon TI-E+C2, Japan). The excitation wavelength was set at 488 nm, and the emission wavelength was set at 522/35 nm. The SEM analysis was conducted as described by Poonguzhali *et al*. (Beattie and Lindow, 1999; Poonguzhali *et al*., 2008) with minor modifications. Leaf tissues were collected and cut into 0.5 cm^2 pieces. The tissues were transferred into a 0.1 M phosphate buffer (PB) containing 2.5% glutaraldehyde and incubated for 40 min at RT followed by 1 h incubation in a 1% osmium tetroxide solution at RT. After three rinses in 0.1 M PB, the fixed tissues were dehydrated in 30, 40, 50, 60, 70, 80, 90 and then 100% ethanol solution. After dehydration, the tissues were freeze-dried and coated with gold–palladium using a Pelco 3 sputter coater (PELCO, USA) and examined under a scanning electron microscope (Nova NanoSEM 230, USA).

Statistical analysis

All the experiments performed in this study were done in three parallels. Results shown in each figure or table were from a single experiment. The results were presented as the mean ± standard deviation (SD) from three or four biological replicates. Statistical differences between the treatments were determined using the one-way ANOVA followed by the Tukey's test using the SPSS Statistics 17.0 software (IBM Corp., New York, USA).

Acknowledgements

This research was supported by the National Key R&D Program of China (2017YFD0200400), the National Science Foundation of China (31701764), Hunan Agricultural Science and Technology Innovation Fund (2017GC04), Hunan Natural Science Foundation (2017JJ3169), and the Hunan Provincial key research and Development Plan (2016NK2199). The grant

agencies had no role in study design, data collection and analysis, the decision to publish, or the preparation of this manuscript.

Conflict of interests

The authors declare no competing financial interests.

Author contributions

PS, ZZ, DZ, XT, JC and LZ designed the experiments and analysed the data. PS, AC, WT, JP and ZZ performed the experiments. XZ, XD, YL and MRH contributed reagents/materials. PS and DZ wrote the paper. The authors want to thank Dr. Xin Shun Ding (The Noble Foundation, Ardmore, USA [retired], for his help during the preparation of this manuscript).

References

Beattie, G.A., and Lindow, S.E. (1999) Bacterial colonization of leaves: a spectrum of strategies. *Phytopathology* **89:** 353–359.

Berg, G. (2009) Plant-microbe interactions promoting plant growth and health: perspectives for controlled use of microorganisms in agriculture. *Appl Microbiol Biotechnol* **84:** 11–18.

Bonaterra, A., Cabrefiga, J., Camps, J., and Montesinos, E. (2007) Increasing survival and efficacy of a bacterial biocontrol agent of fire blight of rosaceous plants by means of osmoadaptation. *FEMS Microbiol Ecol* **61:** 185–195.

Bulgarelli, D., Schlaeppi, K., Spaepen, S., van Themaat, E.V.L., and Schulze-Lefert, P. (2013) Structure and functions of the bacterial microbiota of plants. *Annu Rev Plant Biol* **64:** 807–838.

Duke, K.A., Becker, M.G., Girard, I.J., Millar, J.L., Fernando, W.D., Belmonte, M.F., and Kievit, T.R. (2017) The biocontrol agent *Pseudomonas chlororaphis* PA23 primes *Brassica napus* defenses through distinct gene networks. *BMC Genom* **18:** 467.

Fawzy, Z., El-Magd, M.A., Li, Y., Ouyang, Z., and Hoda, A. (2012) Influence of foliar application by EM "effective microorganisms", amino acids and yeast on growth, yield and quality of two cultivars of onion plants under newly reclaimed soil. *J Agric Sci* **4:** 26–39.

Haefele, D.M., and Lindow, S.E. (1987) Flagellar motility confers epiphytic fitness advantages upon *Pseudomonas syringae*. *Appl Environ Microbiol* **53:** 2528–2533.

Hassani, M.A., Durán, P., and Hacquard, S. (2018) Microbial interactions within the plant holobiont. *Microbiome* **6:** 58.

Hidetada, H., Schaefer, A.L., Greenberg, E.P., and Harwood, C.S. (2012) Anaerobic p-coumarate degradation by *Rhodopseudomonas palustris* and identification of CouR, a MarR repressor protein that binds p-coumaroyl coenzyme A. *J Bacteriol* **194:** 1960–7.

Idi, A., Nor, M.H.M., Wahab, M.F.A., and Ibrahim, Z. (2015) Photosynthetic bacteria: an eco-friendly and cheap tool for bioremediation. *Rev Environ Sci Bio/Technol* **14:** 271–285.

Jiang, C.-H., Huang, Z.-Y., Xie, P., Gu, C., Li, K., Wang, D.-C., *et al*. (2015) Transcription factors WRKY70 and WRKY11 served as regulators in rhizobacterium *Bacillus cereus* AR156-induced systemic resistance to *Pseudomonas syringae* pv. tomato DC3000 in Arabidopsis. *J Exp Bot* **67:** 157–174.

Kembel, S.W., O'Connor, T.K., Arnold, H.K., Hubbell, S.P., Wright, S.J., and Green, J.L. (2014) Relationships between phyllosphere bacterial communities and plant functional traits in a neotropical forest. *Proc Natl Acad Sci USA* **111:** 13715–13720.

Kim, Y.C., Leveau, J., Gardener, B.B.M., Pierson, E.A., Pierson, L.S., and Ryu, C.-M. (2011) The multifactorial basis for plant health promotion by plant-associated bacteria. *Appl Environ Microbiol* **77:** 1548–1555.

Lambais, M.R., Lucheta, A.R., and Crowley, D.E. (2014) Bacterial community assemblages associated with the phyllosphere, dermosphere, and rhizosphere of tree species of the Atlantic forest are host taxon dependent. *Microb Ecol* **68:** 567–574.

Larimer, F.W., Chain, P., Hauser, L., Lamerdin, J., Malfatti, S., Do, L., *et al*. (2004) Complete genome sequence of the metabolically versatile photosynthetic bacterium *Rhodopseudomonas palustris*. *Nat Biotechnol* **22:** 55.

Limoli, D.H., Jones, C.J., and Wozniak, D.J. (2015) Bacterial extracellular polysaccharides in biofilm formation and function. *Microbiol Spectr* **3.**

Limtong, S., and Koowadjanakul, N. (2012) Yeasts from phylloplane and their capability to produce indole-3-acetic acid. *World J Microbiol Biotechnol* **28:** 3323–3335.

Lindemann, A., Pessi, G., Schaefer, A.L., Mattmann, M.E., Christensen, Q.H., Kessler, A., *et al*. (2011) Isovaleryl-homoserine lactone, an unusual branched-chain quorum-sensing signal from the soybean symbiont *Bradyrhizobium japonicum*. *Proc Natl Acad Sci USA* **108:** 16765–16770.

Lindow, S.E., and Brandl, M.T. (2003) Microbiology of the phyllosphere. *Appl Environ Microbiol* **69:** 1875–1883.

Marketon, M.M., Glenn, S.A., Eberhard, A., and González, J.E. (2003) Quorum sensing controls exopolysaccharide production in Sinorhizobium meliloti. *J Bacteriol* **185:** 325–331.

Müller, D.B., Vogel, C., Bai, Y., and Vorholt, J.A. (2016) The plant microbiota: systems-level insights and perspectives. *Annu Rev Genet* **50:** 211–234.

Natacha, B., Miriam, B.M., Martin, A., and Vorholt, J.A. (2014) A synthetic community approach reveals plant genotypes affecting the phyllosphere microbiota. *PLoS Genet* **10:** e1004283.

Niu, D.-D., Liu, H.-X., Jiang, C.-H., Wang, Y.-P., Wang, Q.-Y., Jin, H.-L., and Guo, J.-H. (2011) The plant growth–promoting rhizobacterium *Bacillus cereus* AR156 induces systemic resistance in *Arabidopsis thaliana* by simultaneously activating salicylate-and jasmonate/ethylene-dependent signaling pathways. *Mol Plant Microbe Interact* **24:** 533–542.

Okinaka, Y., Yang, C.-H., Perna, N.T., and Keen, N.T. (2002) Microarray profiling of *Erwinia chrysanthemi* 3937 genes that are regulated during plant infection. *Mol Plant Microbe Interact* **15:** 619–629.

Poonguzhali, S., Madhaiyan, M., Yim, W.-J., Kim, K.-A., and Sa, T.-M. (2008) Colonization pattern of plant root and leaf surfaces visualized by use of green-fluorescent-marked strain of *Methylobacterium suomiense* and its persistence in rhizosphere. *Appl Microbiol Biotechnol* **78:** 1033–1043.

Quiñones, B., Pujol, C.J., and Lindow, S.E. (2004) Regulation of AHL production and its contribution to epiphytic fitness in *Pseudomonas syringae*. *Mol Plant Microbe Interact* **17:** 521–531.

Quiñones, B., Dulla, G., and Lindow, S.E. (2005) Quorum sensing regulates exopolysaccharide production, motility, and virulence in *Pseudomonas syringae*. *Mol Plant Microbe Interact* **18:** 682–693.

Remus-Emsermann, M.N., and Schlechter, R.O. (2018) Phyllosphere microbiology: at the interface between microbial individuals and the plant host. *New Phytol* **218:** 1327–1333.

Sasaki, K., Watanabe, M., Suda, Y., Ishizuka, A., and Noparatnaraporn, N. (2005) Applications of photosynthetic bacteria for medical fields. *J Biosci Bioeng* **100:** 481–488.

Schaefer, A.L., Greenberg, E., Oliver, C.M., Oda, Y., Huang, J.J., Bittan-Banin, G., *et al*. (2008) A new class of homoserine lactone quorum-sensing signals. *Nature* **454:** 595.

Spaepen, S., Vanderleyden, J., and Remans, R. (2007) Indole-3-acetic acid in microbial and microorganism-plant signaling. *FEMS Microbiol Rev* **31:** 425–448.

Su, P., Tan, X., Li, C., Zhang, D., Cheng, J.E., Zhang, S., *et al*. (2017) Photosynthetic bacterium R hodopseudomonas palustris GJ-22 induces systemic resistance against viruses. *Microb Biotechnol* **10:** 612–624.

Tan, C.H., Koh, K.S., Xie, C., Tay, M., Zhou, Y., Williams, R., *et al*. (2014) The role of quorum sensing signalling in EPS production and the assembly of a sludge community into aerobic granules. *ISME J* **8:** 1186.

Von Bodman, S.B., Majerczak, D.R., and Coplin, D.L. (1998) A negative regulator mediates quorum-sensing control of exopolysaccharide production in *Pantoea stewartii* subsp. *stewartii*. *Proc Natl Acad Sci USA* **95:** 7687–7692.

Vorholt, J.A. (2012) Microbial life in the phyllosphere. *Nat Rev Microbiol* **10:** 828–840.

Wilson, M., Hirano, S., and Lindow, S. (1999) Location and survival of leaf-associated bacteria in relation to pathogenicity and potential for growth within the leaf. *Appl Environ Microbiol* **65:** 1435–1443.

Wong, W.-T., Tseng, C.-H., Hsu, S.-H., Lur, H.-S., Mo, C.-W., Huang, C.-N., *et al*. (2014) Promoting effects of a single *Rhodopseudomonas palustris* inoculant on plant growth by *Brassica rapa chinensis* under low fertilizer input. *Microb Environ* **29:** 303–313.

Wu, J., Wang, Y., and Lin, X. (2013) Purple phototrophic bacterium enhances stevioside yield by *Stevia rebaudiana* Bertoni via foliar spray and rhizosphere irrigation. *PLoS ONE* **8:** e67644.

Supporting information

Additional supporting information may be found online in the Supporting Information section at the end of the article.

Appendix S1. Mutant generation.
Table S1. Bacterial strains and plasmids.
Table S2. Primers used for plasmid construction.

